JOURNAL OF APPLIED ELECTROCHEMISTRY 14 (1984) 663–674

Influence of current distribution on electrode potentials in bipolar water electrolysis cells of the 'sandwich' type

J. DIVISEK

Institute of Applied Physical Chemistry, Nuclear Research Centre (KFA), Jülich, Federal Republic of Germany

Received 20 December 1983

The potential and current density distributions in a bipolar electrolytic cell for water electrolysis were computed and the solution given as a matrix product. This makes a rapid and simple evaluation of the load-bearing capacity of such a cell possible, taking into consideration the resistance of the bipolar plate and the supply lines, the reciprocal position and gaps of the current bars and the relative resistance characteristics of the two electrodes. At the same time, the electrochemical process was included by means of Tafel parameters. The variation in these data has been given in a dimensionless form and is discussed in detail.

Nomenclature

a	lower anodic current density ($A\,m^{-2}$)
a_A, a_K	Tafel constants (V)
b	width of the system (m)
b_A, b_K	Tafel constants (V decade^{-1})
C_1, C_2, C_3, C_4 D_1, D_2, D_3, D_4	integral constants
d_A	thickness of the anode (m)
d_B	thickness of the bipolar plate (m)
d_C	thickness of the cathode (m)
d_S	thickness of the conductive bars (m)
E_A, E_C	local anode or cathode potential (V)
E_A^0, E_C^0	anodic or cathodic potential reference point (V)
E_{AC}, E_{KC}	local electrochemical potentials (V)
E_{AC}^0, E_{KC}^0	standard potentials (V)
h	electrode gap (m)
i	electrochemical current density ($A\,m^{-2}$)
I, I_{tot}	total current (A)
I_A, I_C	local current flow through the anode or cathode (A)
I_1, I_2	subcurrents (A)
K	constant (m^{-2})
K_1	constant (V)
K_2	constant ($\Omega\,m^2$)
K_{10}	dimensionless potential constant
L	distance between conductive bars (m)
R_s	supply line resistance (Ω)
R_1, R_2	
s	distance between bipolar plate and electrode (m)
U_A, U_C	dimensionless local anode or cathode potential
ΔU_s	potential difference
x	coordinate length (m)
x_i	a fixed value of x
y	dimensionless standardized length coordinate
y_i	a fixed value of y
z	upper current density ($A\,m^{-2}$)
$\alpha, \beta, \gamma_A, \gamma_C, \delta$	dimensionless parameter, cf. Equations 17a, b, 18a–g
ρ_A	specific electrical resistance of anode ($\Omega\,m$)
ρ_B	specific electrical resistance of bipolar plate ($\Omega\,m$)
ρ_C	specific electrical resistance of cathode ($\Omega\,m$)
ρ_E	specific electrical resistance of electrolyte with diaphragm ($\Omega\,m$)
ρ_S	specific electrical resistance of conductive bars ($\Omega\,m$)

0021–891X/84 $03.00 + .12

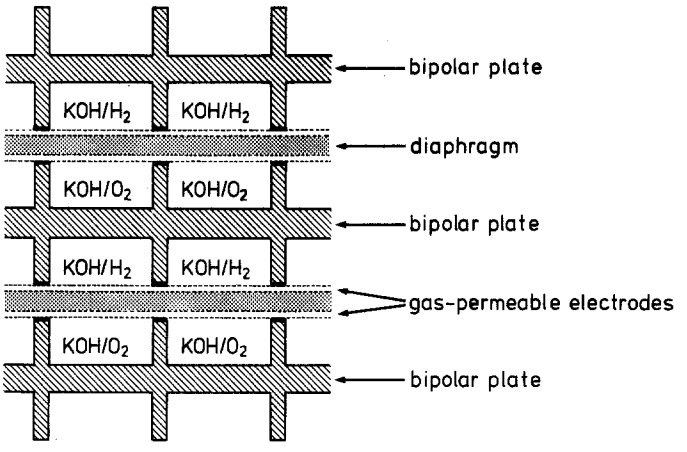

Fig. 1. Principal representation of the functional method of a bipolar electrolyser.

1. Introduction

The increased application of cheap electrochemical hydrogen in the future, requires a reduction of the cell voltage. This can be achieved by a sandwich configuration in which there is a zero gap between catalytically effective electrodes and a thin, non-hydrophobic diaphragm [1, 2].

Sandwich electrolysis cells for alkaline or acid water electrolysis have already been constructed on this principle [3–7]. A very clear illustration of this design principle is given by Costa and Grimes [4] for alkaline water electrolysis and by Lu and Srinivasan [5] for acid electrolysis. It is schematically depicted in Fig. 1. It can, moreover, be shown that by this configuration the influence of bubble formation on the cell voltage is practically negligible, particularly if the diaphragm contains no hydrophobic components [6]. It therefore need not be included in calculating the cell voltage.

In Fig. 1 it can be seen how the electric current flows via contacts in a comb-like arrangement out of the bipolar plate into the catalytically effective electrode; the liquid–gas mixture being able to escape through the gaps between the individual teeth. Both the diaphragm and the catalyst layer must be very thin so that the electrode gaps can be really small. The catalyst layer is connected to the bipolar plate via conductive bars. It can be assumed that the electrolysis process, i.e. the exchange of charge between the solid phase (electrode) and the liquid phase (electrolyte), only takes place in the region of the catalyst layer and that both the comb-like arrangement of the conductive bars as well as the bipolar plate only serve as current suppliers or current distributors for the catalyst layer. Both of these systems (catalyst + current supply) have such a slight layer thickness (particularly the catalyst) that potential differences which can no longer be neglected occur during current flow and have to be included in the designing of the electrolytic cell. This paper is concerned with evaluating the resulting losses.

2. Geometric model and description of the assembly

The following assumptions were made in describing the model:

The two electrodes each consist of a gas-permeable (i.e. open or porous) catalyst layer coupled to a suitable current distribution (Fig. 2). This current distribution consists of the bipolar plate and the conductive bars. The electrodes are separated from each other by a diaphragm h metres in thickness impregnated with electrolyte. The diaphragm with the electrolyte has an average specific electrical resistance of ρ_E. The two electrodes (anode and cathode) have intrinsic thicknesses of d_A and d_C, conductive bars of thickness d_S and bipolar plates of thickness d_B. The distance between the bipolar plate and electrode (i.e. the length of the conductive bars) is s and the distance of the conductive bars from each other is the length L. The whole system has a uniform width b. Let the specific electrical resistances of the anode

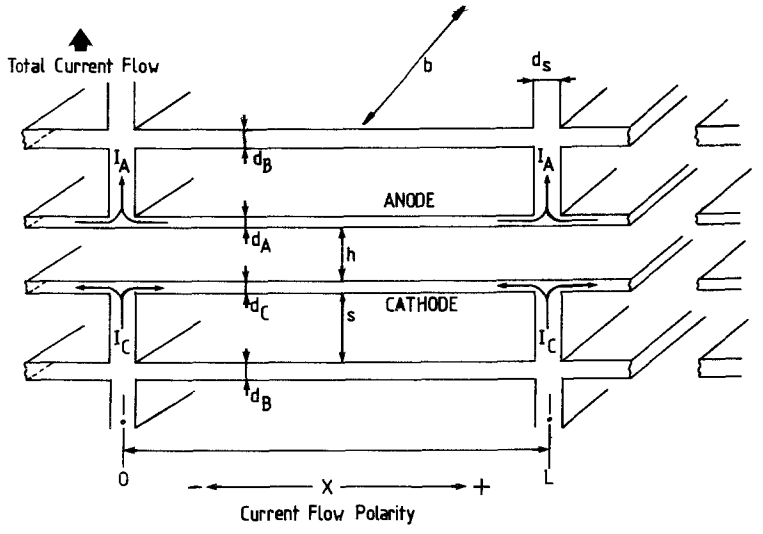

Fig. 2. Model of the configuration.

and cathode be ρ_A or ρ_C and that of the bipolar plates and the bars be ρ_B and ρ_S, respectively, with $\rho_B = \rho_S$.

It is furthermore assumed that:

(a) The end plates of the whole bipolar assembly distribute the current flow very regularly. For this reason periodicity of the potential with the period L can be expected along the coordinate x and the potential remains constant in the direction of width b.

(b) The system is so large that the boundary effects are negligibly small and the individual sections of the length L each behave equivalently towards each other, i.e. periodicity of the characteristics can be expected in the same way as in (a). The anode and cathode are the same size.

(c) d_A, d_C and d_S are all comparable quantities, all significantly smaller than d_B. This latter quantity is, on the other hand, significantly smaller than the dimensions of the whole system, i.e. quantities L and b. One can therefore write $d_A \doteq d_C \doteq d_S \ll d_B \ll L < b$.

(d) The electrode gap h is at most as large as d_B, i.e. $h \ll L \ll b$.

If the zero point of the x coordinate is placed in the cathodic supply bars then the anodic side can be displaced up to the length L until the periodic recurrence of the initial position is achieved again. The picture which then results is depicted in Fig. 3.

Let the cathodic potential reference point E_C^0 be set at zero, i.e. $E_C^0 = 0$. From this point the total

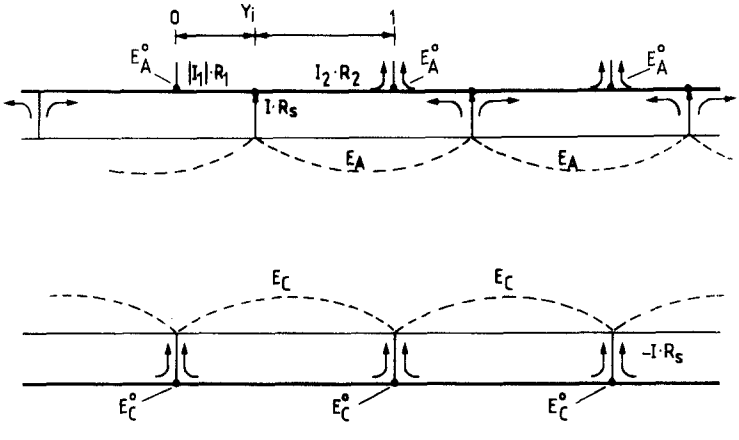

Fig. 3. Current and potential distribution between the bipolar plates.

current, $-I$, flows into the cathode via the cathode bar with resistance R_s. In this way it is divided into the positive and negative direction along coordinate x. The cathode thus experiences a division of the local cathode potential, E_C, as a function of x. The anode bars can be displaced by any length x_i $(0 \leqslant x_i \leqslant L)$. According to the standardization $y = x/L$ this means a displacement by y_i $(0 \leqslant y_i \leqslant 1)$.

On the anode side the total current I is divided into two subcurrents I_1 and I_2. The local potential of the anode, E_A, at the point y_i is removed from the potential location E_A^0 by the difference

$$\Delta E = |I_1| \cdot R_1 + I \cdot R_s = I_2 \cdot R_2 + I \cdot R_s \tag{1}$$

On the other hand, the potential E_A^0 is set at the value $E_C^0 = 0$ for the repetition of the process in the next cell.

Equation 1 is valid on assuming (c), i.e. $d_B \ll L$, otherwise it would be necessary to solve the two-dimensional Laplace equation. With the following relations:

$$R_1 = \frac{L\rho_B y_i}{bd_B} \qquad R_2 = \frac{L\rho_B(1-y_i)}{bd_B} \qquad I = |I_1| + I_2$$

ΔE becomes a function of y, from Equation 1, of the form

$$\Delta E = \frac{L\rho_B I}{bd_B}(y_i - y_i^2) + IR_s \tag{2}$$

with the boundary points

$$y_i = 0 : \Delta E = I \cdot R_s \tag{3a}$$

$$y_i = 1 : \Delta E = I \cdot R_s \tag{3b}$$

An appropriate assumption about the type of differences in the local potentials $(E_A - E_C)$ must also be made before actually computing the current distribution. The potentials of the two electrodes, anode and cathode, are characterized in alkaline water electrolysis by the usual logarithmic, not transport-inhibited dependence, which can be formulated as

$$E_{AC} - E_{AC}^0 = a_A + b_A \log i \quad > 0 \tag{4a}$$

$$E_{KC} - E_{KC}^0 = a_K - b_K \log |i| \quad < 0 \tag{4b}$$

where $a_{A,K}$, $b_{A,K}$ are the usual Tafel constants and i is the electrochemical current density ($A\,m^{-2}$).

On the left side of the equations are electrochemical overvoltages which are to be understood as the difference in the potential measured against a suitable reference electrode. The relation

$$E_A - E_C = E_{AC} - E_{KC} + \rho_E h|i| \tag{5}$$

is valid for the difference in local potentials $(E_A - E_C)$ or with Equations 4a, b

$$E_A - E_C = (E_{AC}^0 - E_{KC}^0 + a_A - a_K) + (b_A + b_K) \log |i| + \rho_E h|i| \tag{6}$$

Equation 6 has the form

$$E_A - E_C = K_1 + K_2 \log |i| + \rho_E h|i| \tag{7}$$

with constants K_1 and K_2.

The quantity $\log |i|$ can be meaningfully linearized by a suitable approximation. The nature of this approximation depends largely on the current density range under investigation. The current densities of technical interest for modern water electrolysis are in a relatively wide range, between 4000 and 10 000 $A\,m^{-2}$, the profitability optimum being only between 4000 and 5000 $A\,m^{-2}$ [2]. If the major interest is in this optimum then the differential approximation by breaking off the Taylor series after the second term is suitable. In this case Equation 6 has the form

$$E_A - E_C = K_1 + K_2 i \tag{8}$$

with

$$K_1 = E_{AC}^0 - E_{KC}^0 + a_A - a_K + (b_A + b_K)\left(\log i_a - \frac{1}{2.303}\right) \tag{9a}$$

$$K_2 = \frac{b_A + b_K}{2.303\, i_a} + \rho_E h \tag{9b}$$

where $i > 0$ is the anodic current density (equal to the cathodic $|i|$) and i_a is the lower anodic current density of the current density interval being studied.

The integral approximation seems more meaningful if one is interested in current densities in a broader range than the profitability optimum. This approximation results by substituting an isohedral triangle for the integral

$$\int_a^z (\ln x - \ln a)\, dx \tag{10}$$

The direction of its hypotenuse then approximates to the course of the function. In this case the constants K_1 and K_2 have the form

$$K_1 = E^0_{AC} - E^0_{KC} + a_A - a_K + (b_A + b_K)\left[\log a - \frac{2a\int_a^z (\ln x - \ln a)\, dx}{2.303(z-a)^2}\right] \tag{11a}$$

$$K_2 = \frac{2(b_A + b_K)\int_a^z (\ln x - \ln a)\, dx}{2.303(a-z)^2} + \rho_E h \tag{11b}$$

The expressions $a = i_a$, $z = i_z$ contained in these formulae are the current densities at the boundary of the interval under investigation.

3. Computation of the system

The current flow $I_{A,C}$ within the electrodes along coordinate x is subject to Ohm's law (cf. Fig. 2).

$$I_A = \frac{b d_A}{\rho_A}\frac{dE_A}{dx} \qquad I_C = \frac{b d_C}{\rho_C}\frac{dE_C}{dx} \tag{12}$$

The electrochemical current density i (cf. Equations 4a, b) is defined as

$$i = \frac{1}{b}\frac{dI_{A,C}}{dx} \tag{13}$$

That $i_A > 0$ is true of the anodic current density i_A and that $i_C < 0$ is true of the cathodic current density; $i_A = |i_C|$ at the same point x according to Assumption (b), i.e.

$$\frac{dI_A}{dx} = -\frac{dI_C}{dx} \tag{14}$$

The relations

$$\frac{dI_A}{dx} = \frac{b d_A}{\rho_A}\frac{d^2E_A}{dx^2} \qquad \frac{dI_C}{dx} = \frac{b d_C}{\rho_C}\frac{d^2E_C}{dx^2} \tag{15}$$

are obtained by differentiating Equation 12. The following equations result by combining Equations 8, 13–15

$$\frac{d^2E_A}{dx^2} = (E_A - E_C)\frac{\rho_A}{K_2 d_A} - \frac{K_1 \rho_A}{K_2 d_A} \tag{16a}$$

$$\frac{d^2E_C}{dx^2} = -(E_A - E_C)\frac{\rho_C}{K_2 d_C} + \frac{K_1 \rho_C}{K_2 d_C} \tag{16b}$$

The solution of this differential equation system is

$$E_A = C_1 \exp[(K)^{1/2}x] + C_2 \exp[-(K)^{1/2}x] + C_3x + C_4 \tag{17a}$$

$$E_C = -\alpha C_1 \exp[(K)^{1/2}x] - \alpha C_2 \exp[-(K)^{1/2}x] + C_3x + C_4 - K_1 \tag{17b}$$

where $\alpha = \rho_C d_A/\rho_A d_C, K = [(\rho_A/d_A) + (\rho_C/d_C)](1/K_2)$ and C_i $(i = 1\text{–}4)$ are arbitrary constants.

Before the boundary conditions are formulated it seems meaningful to carry out a suitable dimensionless standardization, which is particularly advantageous for a numerical evaluation. For this reason the following dimensionless parameters are introduced:

$$y = \frac{x}{L} \qquad \text{a fixed value } y_i = \frac{x_i}{L} \tag{18a}$$

$$U_A = \frac{E_A}{E_A^0 - E_C^0} = \frac{E_A}{E_A^0} \qquad U_C = \frac{E_C}{E_A^0 - E_C^0} = \frac{E_C}{E_A^0} \tag{18b}$$

$$\beta = \frac{\rho_B d_A}{\rho_A d_B} \qquad \gamma_A = \frac{s\rho_s d_A}{L\rho_A d_s} \qquad \gamma_C = \frac{s\rho_s d_C}{L\rho_C d_s} \tag{18c}$$

$$\delta = L(K)^{1/2} = \delta_1(1+\alpha)^{1/2} \tag{18d}$$

$$K_{10} = \frac{K_1}{E_A^0} \tag{18e}$$

$$\Delta U = \frac{\Delta E}{E_A^0} = [\beta(y_i - y_i^2) + \gamma_A]\left[\left(\frac{dU_A}{dy}\right)_{y_i^-} - \left(\frac{dU_A}{dy}\right)_{y_i^+}\right] \tag{18f}$$

$$\Delta U_s = \frac{|I|R_s}{E_A^0} = \gamma_C\left[\left(\frac{dU_C}{dy}\right)_{0^+} - \left(\frac{dU_C}{dy}\right)_{1^-}\right] \tag{18g}$$

In principle a difference should be made between $y_i = 0$ and $0 < y_i < 1$. If $y_i = 0$ then

$$U_A = C_1 \exp(\delta y) + C_2 \exp(-\delta y) + C_3 y + C_4 \tag{19a}$$

$$U_C = -\alpha C_1 \exp(\delta y) - \alpha C_2 \exp(-\delta y) + C_3 y + C_4 - K_{10} \tag{19b}$$

result from Equations 17a, b taking Equations 18a–g into consideration. The corresponding boundary conditions are:

$$y = 0 \qquad U_A = 1 - \Delta U \tag{20a}$$

$$U_C = \Delta U_s \tag{20b}$$

$$y = 1 \qquad U_A = 1 - \Delta U \tag{20c}$$

$$U_C = \Delta U_s \tag{20d}$$

(Since C_i are arbitrary they can be designated by the same symbols as in Equations 17a, b.) By combining Equations 3a, b, 19a, b and 20a–d, the constants C_i are found to be

$$C_1 = \frac{(K_{10}-1)[1-\exp(-\delta)]}{4\gamma_A\delta[2-\exp(\delta)-\exp(-\delta)] + [\exp(-\delta)-\exp(\delta)](1+\alpha)} \tag{21a}$$

$$C_2 = \frac{(K_{10}-1)[\exp(\delta)-1]}{4\gamma_A\delta[2-\exp(\delta)-\exp(-\delta)] + [\exp(-\delta)-\exp(\delta)](1+\alpha)} \tag{21b}$$

$$C_3 = 0 \tag{21c}$$

$$C_4 = \frac{(\alpha+K_{10})[\exp(-\delta)-\exp(\delta)] - 2\gamma_A\delta[\exp(\delta)+\exp(-\delta)-2](1+K_{10})}{4\gamma_A\delta[2-\exp(\delta)-\exp(-\delta)] + [\exp(-\delta)-\exp(\delta)](1+\alpha)} \tag{21d}$$

If $0 < y_i < 1$ then the following conditions must be taken into consideration: the functions E_A and E_C, or U_A and U_C are continuous but their derivatives at points $0, y_i$ and 1 are not. The total interval (0, 1) is therefore split into two subintervals $(0, y_i)$ and $(y_i, 1)$ with a simultaneous division of the functions in Equations 19a, b. The following is accordingly obtained with the dimensionless parameters already introduced:

interval $(0, y_i)$

$$U_A = C_1 \exp(\delta y) + C_2 \exp(-\delta y) + C_3 y + C_4 \tag{22a}$$

$$U_C = -\alpha C_1 \exp(\delta y) - \alpha C_2 \exp(-\delta y) + C_3 y + C_4 - K_{10} \tag{22b}$$

interval $(y_i, 1)$

$$U_A = D_1 \exp(\delta y) + D_2 \exp(-\delta y) + D_3 y + D_4 \tag{22c}$$

$$U_C = -\alpha D_1 \exp(\delta y) - \alpha D_2 \exp(-\delta y) + D_3 y + D_4 - K_{10} \tag{22d}$$

Differences must be made in the boundary conditions between the left-hand and right-hand derivatives.

$$y = 0 \qquad U_C = \Delta U_s \tag{23a}$$

$$U_A = (U_A)_0 = (U_A)_1 \tag{23b}$$

$$\left(\frac{dU_A}{dy}\right)_{0^+} = \left(\frac{dU_A}{dy}\right)_{1^-} \tag{23c}$$

The latter two boundary conditions result from the periodicity of the properties according to Assumptions (a) and (b).

$$y = y_i \qquad (U_A)_{y_i^-} = 1 - \Delta U \tag{24a}$$

$$(U_A)_{y_i^+} = 1 - \Delta U \tag{24b}$$

$$(U_C)_{y_i^-} = (U_C)_{y_i^+} \tag{24c}$$

$$\left(\frac{dU_C}{dy}\right)_{y_i^-} = \left(\frac{dU_C}{dy}\right)_{y_i^+} \tag{24d}$$

$$y = 1 \qquad U_C = \Delta U_s \tag{25a}$$

$$U_A = (U_A)_1 = (U_A)_0 \tag{25b}$$

$$\left(\frac{dU_A}{dy}\right)_{1^-} = \left(\frac{dU_A}{dy}\right)_{0^+} \tag{25c}$$

With the notation $\beta(y_i - y_i^2) + \gamma_A = \omega$, $\gamma_C = \gamma$, the system of equations from Equations 22a–d to Equation 25a–c can be written as a matrix product in a suitable form for numerical computation as given in Equation 26.

$$\begin{bmatrix}
-\alpha+\alpha\gamma\delta & -\alpha-\alpha\gamma\delta & -\gamma & 1 & -\alpha\gamma\delta e^{\delta} & \alpha\gamma\delta e^{-\delta} & \gamma & 0 \\
1 & 1 & 0 & 1 & -e^{\delta} & -e^{-\delta} & -1 & -1 \\
\delta & -\delta & 1 & 0 & -\delta e^{\delta} & \delta e^{-\delta} & -1 & 0 \\
(1+\omega\delta)e^{\delta y_i} & (1-\omega\delta)e^{-\delta y_i} & \omega+y_i & 1 & -\omega\delta e^{\delta y_i} & \omega\delta e^{-\delta y_i} & -\omega & 0 \\
\omega\delta e^{\delta y_i} & -\omega\delta e^{-\delta y_i} & \omega & 0 & (1-\omega\delta)e^{\delta y_i} & (1+\omega\delta)e^{-\delta y_i} & y_i-\omega & 1 \\
-\alpha e^{\delta y_i} & -\alpha e^{-\delta y_i} & y_i & 1 & \alpha e^{\delta y_i} & \alpha e^{-\delta y_i} & -y_i & -1 \\
-\alpha\delta e^{\delta y_i} & \alpha\delta e^{-\delta y_i} & 1 & 0 & \alpha\delta e^{\delta y_i} & -\alpha\delta e^{-\delta y_i} & -1 & 0 \\
\alpha\gamma\delta & -\alpha\gamma\delta & -\gamma & 0 & -\alpha(1+\gamma\delta)e^{\delta} & \alpha(\gamma\delta-1)e^{-\delta} & 1+\gamma & 1
\end{bmatrix}
\cdot
\begin{bmatrix} C_1 \\ C_2 \\ C_3 \\ C_4 \\ D_1 \\ D_2 \\ D_3 \\ D_4 \end{bmatrix}
=
\begin{bmatrix} K_{10} \\ 0 \\ 0 \\ 1 \\ 1 \\ 0 \\ 0 \\ K_{10} \end{bmatrix} \tag{26}$$

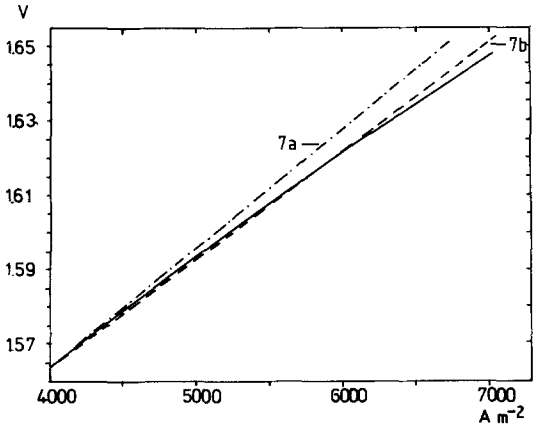

Fig. 4. Current–voltage curves of advanced alkaline water electrolysis.

The coefficients C_i, D_i, and thus also the equations system in Equations 22a–d, are simply calculated via determinant formation.

4. Discussion of results

The accuracy of the whole procedure discussed here depends essentially on how well the approximation of Equation 7 is given by Equation 8. This is shown in Fig. 4.

In this figure, the curve drawn in full represents a sector of the current–voltage curve of advanced alkaline water electrolysis (AWE), which is in experimental operation at the Nuclear Research Centre KFA Jülich [8]. Electrolysis takes place at 100°C in 10 N KOH. The logarithmic curve is described according to Equation 6 or 7 by the following values:

$$E^0_{AC} - E^0_{KC} = 1.1950, \qquad a_A = -0.035, \qquad a_K = 0.1850,$$

$$b_A = 0.075, \qquad b_K = 0.070, \qquad \rho_E h = 1.65 \times 10^{-5}\,\Omega\,m^2$$

According to Equation 11a, b the values $K_1 = 1.4459$ and $K_2 = 2.934 \times 10^{-5}$, and according to Equation 9a, b $K_1 = 1.4343$ and $K_2 = 3.224 \times 10^{-5}$ which correspond to these conditions. As can be seen from Fig. 4, a better agreement with the logarithmic curve is achieved by the integral approximation of Equation 11a, b than with the differential approximation of Equations 9a, b. The functional values are approximated with an accuracy of better than 4% with Equation 11a, b. The agreement is even better in the narrower current density range. For this reason, only the approximation according to Equation 11a, b is used in the following and computed with corresponding K values.

The principal potential course $U_{A,C}$ is shown in Fig. 5 with two different y_i values. The curves reflect

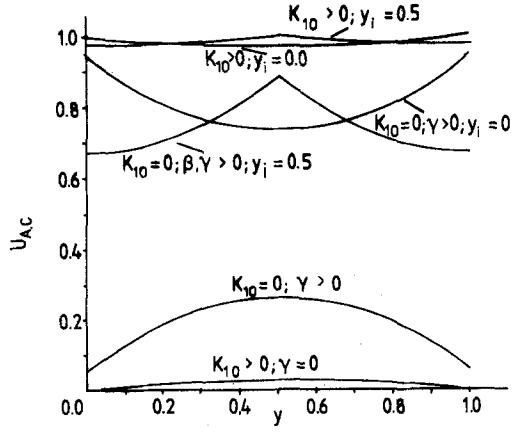

Fig. 5. Principal potential course U_A, U_C at $y_i = 0$ and $y_i = 0.5$.

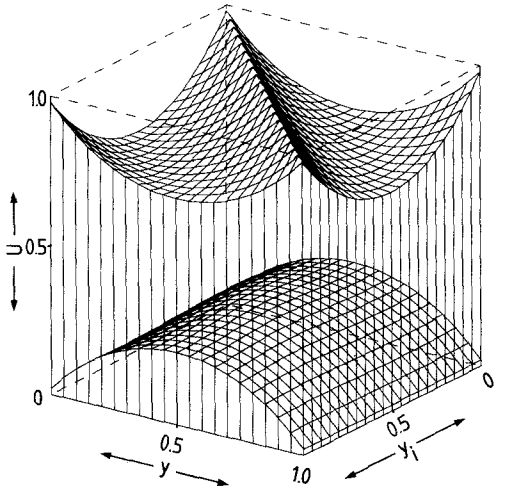

Fig. 6. Anodic and cathodic potential course U_A, U_C without including the electrochemical process, $\alpha = 1.00$, $\beta = 0.02$, $\gamma_A = 0.01$, $K_{10} = 0.00$, $\delta_1 = 1.75$.

various influences. The distance of the corner points from 1 or 0 is thus a measure of the size of the potential drop in the bipolar plate and the supply lines. It is influenced by β and γ. Consideration of the electrochemical process (Tafel straight line) means that $K_1 > 0$ and $K_2 > \rho_E h$. It flattens the curve, i.e. as a whole less current passes through the cell.

Equation 13 is valid for the electrochemical current density i. Accordingly, the total current passing through the electrode section $0 \leqslant x \leqslant L$ $(0 \leqslant y \leqslant 1)$ can be expressed by the relation

$$I_{tot} = bL \int_0^1 i \, dy \tag{27}$$

or with Equation 8

$$I_{tot} = \frac{bLE_A^0}{K_2} \int_0^1 (U_A - U_C - K_{10}) \, dy \tag{28a}$$

$$I_{tot} = \frac{bLE_A^0(1+\alpha)}{\delta K_2} \{C_1[\exp(\delta y_i) - 1] + C_2[1 - \exp(-\delta y_i)] + D_1[\exp(\delta) - \exp(\delta y_i)] + D_2[\exp(-\delta y_i) - \exp(-\delta)]\} \tag{28b}$$

This current I_{tot} is, amongst other aspects, a function of y_i. The value y_i is a measure of the reciprocal shift of the conductive bars on the anodic and cathodic sides of the bipolar plate.

A functional dependence of the two potentials U_A and U_C on y_i is shown by Fig. 6. The input parameter data resemble the characteristics of an electrolytic cell for alkaline water electrolysis firstly without considering the electrochemical process (Tafel plots). The cell under consideration has two equivalent porous electrodes which are directly connected to the separator with a zero gap [6]. It can be seen in Fig. 6 that a modification of y_i, i.e. the reciprocal position of the anodic supply lines, only slightly changes the total potential profile, but it does change the position of the potential peaks. Two important properties are required of a well-functioning electrochemical cell: first of all at a given total potential E_A^0 (here identical with the total voltage) as much current as possible should flow through the cell and secondly the current density distribution along the y-coordinate should be as uniform as possible. These two aspects can be taken from Fig. 6; they are included in Figs. 7 and 8.

The dependence of the total current $I_{tot}/I_{tot,o}$ is represented as a function of y_i in Fig. 7. It becomes apparent here that in the case of $\beta = \gamma_{A,C} = 0$ also, the maximum current flow $I_{tot,o}$ is at $y_i = 0$ (or $y_i = 1$) and the minimum at $y_i = 0.5$. In contrast it can be seen from Fig. 8a that the most uniform current density distribution is at $y_i = 0.5$ and relatively, the largest irregularities occur at $y_i = 0$ or 1. These conclusions from Fig. 8a are analogous to Robertson's treatment [9] where $y_i = 0.5$ corresponds to his case of a single cell unit with current supply lines on the inverse ends of the cell.

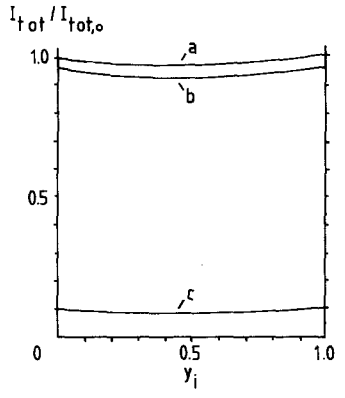

Fig. 7. Relative total current as a function of the shift in the supply lines y_i. (a) Only the cell with parameters $\alpha = 1.00, \beta = 0.00, \gamma_A = 0.00, K_{10} = 0.00, \delta_1 = 1.75$; (b) only the cell with parameters: $\alpha = 1.00, \beta = 0.02, \gamma_A = 0.01, K_{10} = 0.00, \delta_1 = 1.75$; (c) electrolysis also included: $\alpha = 1.00, \beta = 0.02, \gamma_A = 0.01, K_{10} = 0.85, \delta_1 = 1.30$.

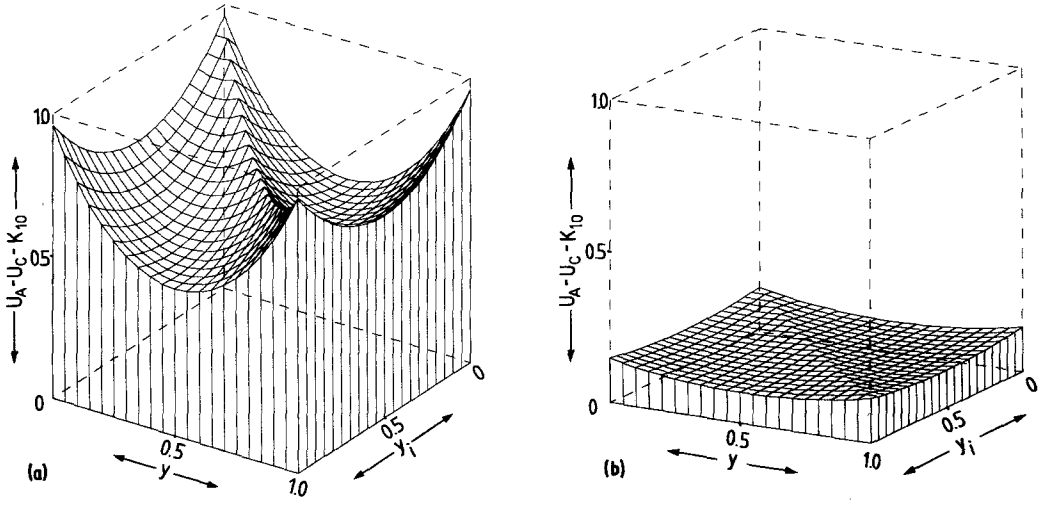

Fig. 8. Difference in potential as criterion of current density distribution. (a) Only the cell with parameters: $\alpha = 1.00, \beta = 0.02, \gamma_A = 0.01, K_{10} = 0.00, \delta_1 = 1.75$; (b) electrolysis also included: $\alpha = 1.00, \beta = 0.02, \gamma_A = 0.01, K_{10} = 0.85, \delta_1 = 1.30$.

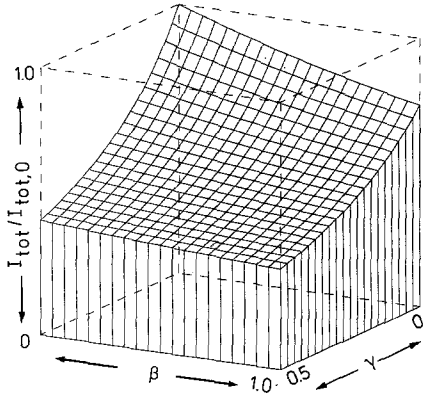

Fig. 9. Relative total current as a function of the resistances of the bipolar plate and the supply lines: $\alpha = 1.00, K_{10} = 0.85, \delta_1 = 1.30, y_i = 0.5$.

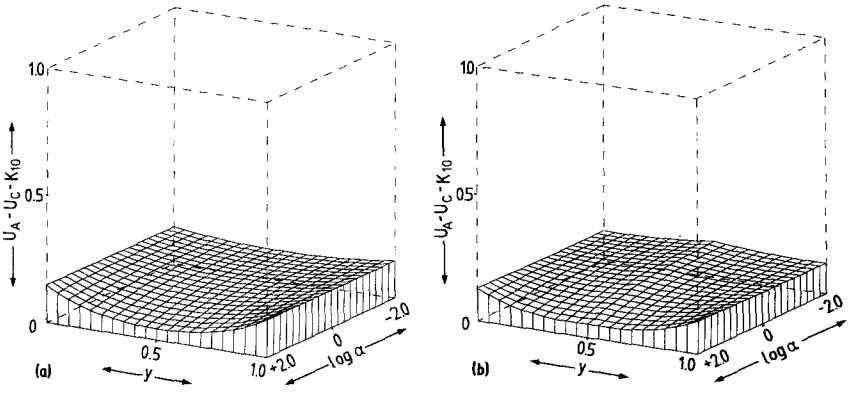

Fig. 10. Differences in potential as a criterion of current density distribution including electrolysis. (a) Anodic and cathodic supply lines directly opposite: $\beta = 0.02$, $\gamma_A = 0.01$, $K_{10} = 0.85$, $\delta_1 = 1.30$, $y_i = 0.00$; (b) supply lines each shifted by half the distance: $\beta = 0.02$, $\gamma_A = 0.01$, $K_{10} = 0.85$, $\delta_1 = 1.30$, $y_i = 0.50$.

Computation of the current density distribution of the same cell as in Fig. 6, but including the electrochemical process (water electrolysis) is shown in Figs. 7 (at c) and 8b. An analogous picture results, i.e. the most uniform current distribution is at $y_i = 0.5$, whereas the greatest total current is at $y_i = 0$ or 1. The available volume of current flowing through the electrolytic cell in this case is significantly smaller than in Fig. 8a.

A further important aspect is the question of losses caused by the bipolar plate and current supply lines. These data are included in the parameters $\gamma_{A,C}$ and β, and shown by Fig. 9. The function $I_{tot}/I_{tot,o}$ was computed for $y_i = 0.5$. The course at $y_i = 0$ results from the cut at $\beta = 0$. The quantity $I_{tot,o}$ is the current at $\beta = \gamma_A = 0$. (I_{tot} is defined by Equation 28a, b.)

The previous data showed relations at geometrically identically designed electrodes: anode and cathode. However, these can be constructed differently, i.e. they can be of different thickness and electrical resistance. This is taken into consideration by changing the parameter α as shown in Fig. 10.

With the designation $I_{tot}/L = i_{tot}$, the dependence of $i_{tot}/i_{tot,o}$ on δ and y_i is finally shown in Fig. 11. The quantity $i_{tot,o}$ is here the current i_{tot} at $\delta = y_i = 0$. The function thus specified represents the same dependence as the electrode utilization factor already used by Robertson [9] and Scott [10]. As can be seen in Fig. 11, enlargement of the parameter δ means a more perceptible deterioration of this factor at $y_i = 0.5$ than e.g. at $y_i = 0$.

In general the following may be stated. The highest current flow through the electrolytic cell at a given total voltage is achieved if the current supply lines are placed directly against each other. This arrangement becomes all the more advantageous as the larger the resistances of the cell components are, the more unsymmetrical the electrode properties and the larger the line gaps. However, it causes a more unfavourable current density distribution and consequently less possibility of power load on the cell. In designing the cell it must therefore be decided from case to case which properties are to be preferred.

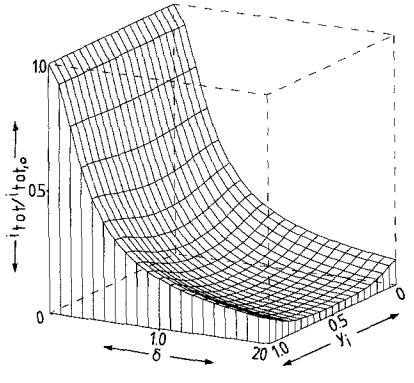

Fig. 11. Electrode utilization factors: $\alpha = 1.00$, $\beta = 0.00$, $\gamma_A = 0.00$, $K_{10} = 0.00$.

Acknowledgement

The author wishes to thank Professor H. W. Nürnberg for kindly supporting this work.

References

[1] J. Divisek and H. W. Nürnberg, 'Moderne Elektrolytische Verfahren zur Wasserstoffherstellung, Jahresbericht 1981/82', S.55, KFA, Jülich (1982).
[2] H. W. Nürnberg, in 'Hydrogen as a Energy Carrier', edited by G. Imarisio and A. S. Strub, D. Reidel Publishing Co. (1983) p. 16.
[3] J. Fischer, H. Hofmann, G. Luft and H. Wendt, *AIChE J.* **26** (1980) 794.
[4] R. L. Costa and P. G. Grimes in 'Chemical Engineering Progress Symposia Series' edited by M. Steinberg and J. H. Holmes, Vol. 63. (American Institute of Chemical Engineers, 1967) p. 45.
[5] P. W. T. Lu and S. Srinivasan, *J. Appl. Electrochem.* **9** (1979) 269.
[6] J. Divisek and H. Schmitz, *Int. J. Hydrogen Energy* **7** (1982) 703.
[7] H. Vandenborre, R. Leysen and L. H. Baetslé, *ibid.* **5** (1980) 165.
[8] H. Smitz and J. Mergel, unpublished results.
[9] P. M. Robertson, *Electrochim. Acta* **22** (1977) 411.
[10] K. Scott, *ibid.* **28** (1983) 133.